Time-Resolved Gas-Phase Kinetic and Quantum Chemical Studies of Reactions of Silylene with Chlorine-Containing Species. 1. HCl

Rosa Becerra

Instituto de Quimica-Fisica "Rocasolano", C.S.I.C., C/Serrano 119, 28006 Madrid, Spain

J. Pat Cannady

Dow Corning Corporation, P.O. Box 995, Mail 128, Midland, Michigan, 48686-0995

Robin Walsh*

Department of Chemistry, University of Reading, Whiteknights, P.O. Box 224, Reading, RG6 6AD, UK

Received: November 27, 2003; In Final Form: February 19, 2004

Time-resolved kinetic studies of the reaction of silylene, SiH_2, generated by laser flash photolysis of phenylsilane, have been carried out to obtain rate constants for its bimolecular reaction with HCl. The reaction was studied in the gas phase at 10 Torr total pressure in SF_6 bath gas, at five temperatures in the range of 296−611 K. The second-order rate constants fitted the Arrhenius equation: $\log(k/\mathrm{cm^3\ molecule^{-1}\ s^{-1}}) = (-11.51 \pm 0.06) + (1.92 \pm 0.47\ \mathrm{kJ\ mol^{-1}})/RT\ln 10$ Experiments at other pressures showed that these rate constants were unaffected by pressure in the range of 10−100 Torr, but showed small decreases in value of no more than 20% (±10%) at 1 Torr, at both the highest and lowest temperatures. The data are consistent with formation of an initial weakly bound donor−acceptor complex, which reacts by two parallel pathways. The first is by chlorine-to-silicon H-shift to make vibrationally excited chlorosilane, SiH_3Cl^*, which yields HSiCl by H_2 elimination from silicon. In the second pathway, the complex proceeds via H_2 elimination (4-center process) to make chlorosilylene, HSiCl, directly. This interpretation is supported by ab initio quantum calculations carried out at the G3 level which reveal the direct H_2 elimination route for the first time. RRKM modeling predicts the approximate magnitude of the pressure effect but is unable to determine the proportions of each pathway. The experimental data agree with the only previous measurements at room temperature. Comparisons with other reactions of SiH_2 are also drawn.

Introduction

Silylenes are of importance because they are implicated in the thermal and photochemical breakdown mechanisms of silicon hydrides and organosilanes, as well as being key intermediates in chemical vapor deposition (CVD). Time-resolved kinetic studies, carried out in recent years, have shown that the simplest silylene, SiH_2, reacts rapidly and efficiently with many chemical species.[1,2] Examples of its reactions include Si−H bond insertions and C═C and C≡C π-bond additions.[3] SiH_2 also has a great affinity for electronegative elements and will react with lone pair donor species containing the elements of N, O, F, P, S, and Cl among others.[4] We, and others, have recently studied the kinetics of its reactions with O-donor molecules, H_2O,[5,6] CH_3OH (CD_3OD),[5] Me_2O,[7,8] Me_2CO,[9] MeCHO,[10,11] N_2O,[12] CO,[13] and CO_2.[14] Because of the importance of chlorosilanes and routes to their formation in the organosilicon industry,[15] we have now turned our attention to reactions of SiH_2 with Cl-containing molecules. We report here the combined results of an experimental kinetic study and theoretical calculations of the energy surface for the reaction of SiH_2 with HCl.

The first and only direct rate study of this reaction was carried out by Chu, Beach, Estes, and Jasinski[16] (CBEJ) who found a weakly pressure dependent reaction (over the range of 1−10 Torr in He) with a rate constant value of $(7.5 \pm 1.0) \times 10^{-12}$ cm^3 molecule^{-1} s^{-1} at 9.5 Torr at room temperature. CBEJ[16] pointed out that a weakly pressure dependent reaction implies incomplete collisional stabilization of the vibrationally excited SiH_3Cl^* initially formed by insertion of SiH_2 into the H−Cl bond. They also suggested that decomposition of SiH_3Cl^* into $SiHCl + H_2$ could not be too rapid or this would also remove the pressure dependence. Theoretical calculations, carried out by Raghavachari, Chandrasekhar, Gordon, and Dykema[4] (RCGD), and Su and Schlegel,[17] indicate that the formal insertion process consists of the initial formation of a donor−acceptor complex, $H_2Si\cdots ClH$, followed by its rearrangement to SiH_3Cl. The well depth of the complex lies in the range of −8 to −29 kJ mol^{-1} and the barrier to rearrangement in the range of −1 to + 25 kJ mol^{-1}, depending on the level of calculation. The existence of a real barrier would imply a positive activation energy for the reaction. We therefore thought it worthwhile to extend the kinetic measurements of CBEJ[16] to higher temperatures in order to measure the activation energy and to explore a wider range of pressures. In order to try to understand the mechanism more fully, we also decided to reinvestigate the energy surface at a higher level of theory than the earlier studies of RCGD[4] and Su and Schlegel.[17]

Experimental Section

Equipment, Chemicals, and Method. The apparatus and equipment for these studies have been described in detail

10.1021/jp037630i CCC: $27.50

previously.[18,19] Only essential and brief details are therefore included here. SiH_2 was produced by the 193 nm flash photolysis of phenylsilane ($PhSiH_3$) using a Coherent Compex 100 exciplex laser. Photolysis pulses were fired into a variable temperature quartz reaction vessel with demountable windows, at right angles to its main axis. SiH_2 concentrations were monitored in real time by means of a Coherent 699-21 single-mode dye laser pumped by an Innova 90-5 argon ion laser and operating with rhodamine 6G. The monitoring laser beam was multipassed 36 times along the vessel axis, through the reaction zone, to give an effective path length of 1.5 m. A portion of the monitoring beam was split off before entering the vessel for reference purposes. The monitoring laser was tuned to 17 259.50 cm^{-1}, corresponding to a known strong vibration−rotation transition[19,20] in the SiH_2 $A(^1B_1) \leftarrow X(^1A_1)$ absorption band. Light signals were measured by a dual photodiode/differential amplifier combination, and signal decays were stored in a transient recorder (Datalab DL910) interfaced to a BBC microcomputer. This was used to average the decays of between 5 and 20 photolysis laser shots (at a repetition rate of 0.5 or 1 Hz). The averaged decay traces were processed by fitting the data to an exponential form using a nonlinear least-squares package. This analysis provided the values for first-order rate coefficients, k_{obs}, for removal of SiH_2 in the presence of known partial pressures of substrate gas.

Gas mixtures for photolysis were made up, containing between 1.3 and 5.3 mTorr of $PhSiH_3$, 0−4 Torr of HCl, and inert diluent (SF_6) up to total pressures of between 10 and 100 Torr. Pressures were measured by capacitance manometers (MKS, Baratron). All gases used in this work were frozen and rigorously pumped to remove any residual air prior to use. $PhSiH_3$ (99.9%) was obtained from Ventron-Alfa (Petrarch). HCl (99.9%) was from Aldrich. Sulfur hexafluoride, SF_6, (no GC-detectable impurities) was from Cambrian Gases.

Ab Initio Calculations. The electronic structure calculations were performed with the Gaussian 98 software package.[21] All structures were determined by energy minimization at the MP2 = Full/6-31G(d) level. Transition state structures were characterized as first-order saddle points by calculation of the Hessian matrix. Stable structures, corresponding to energy minima, were identified by possessing no negative eigenvalues of the Hessian, while transition states were identified by having one and only one negative eigenvalue. The standard Gaussian-3 (G3) compound method[22] was employed to determine final energies for all local minima. For transition states four single-point energy determinations were carried out at the MP2 geometry, viz: QCISD(T)/6-31G(d), MP4/6-31+G(d), MP4/6-31G(2df,p), and optimized MP2 = full/GTlarge, and the values were combined according to the G3 procedure.[22] The identities of the transition state structures were verified by calculation of intrinsic reaction coordinates[23] (IRC) at the MP2 = Full/6-31G(d) or B3LYP/6-31G(d) levels. Reaction barriers were calculated as differences in G3 enthalpies at 298.15 K. Where required, harmonic frequencies were obtained from the values calculated at the HF/6-31G(d) level adjusted by the correction factor 0.893 appropriate to this level.[24]

Results

Kinetics. Preliminary experiments established that, for a given reaction mixture, decomposition decay constants, k_{obs}, were not dependent on the exciplex laser energy (50−70 mJ/pulse, routine variation) or number of photolysis laser shots (up to 20 shots). The constancy of k_{obs} (5 shot averages) showed no effective depletion of reactants. Higher pressures of precursor were required at the higher temperature because signal intensities decreased with increasing temperature. However, for the purposes of rate constant measurement at a given temperature, the $PhSiH_3$ pressure was kept fixed. At each temperature of study, a series of experiments was carried out to investigate the dependence of k_{obs} on HCl pressure (at least six different values). The results of these experiments are shown in Figure 1, where good linear fits were obtained, as expected for second-order kinetics. The second-order rate constants derived from the gradients of these plots by least-squares fitting are shown in Table 1. The error limits are single standard deviations and are fairly small. It is clear that the rate constants decrease with increasing temperature (just as has been found in other similar SiH_2 reactions[6,9−13,18,25−30]).

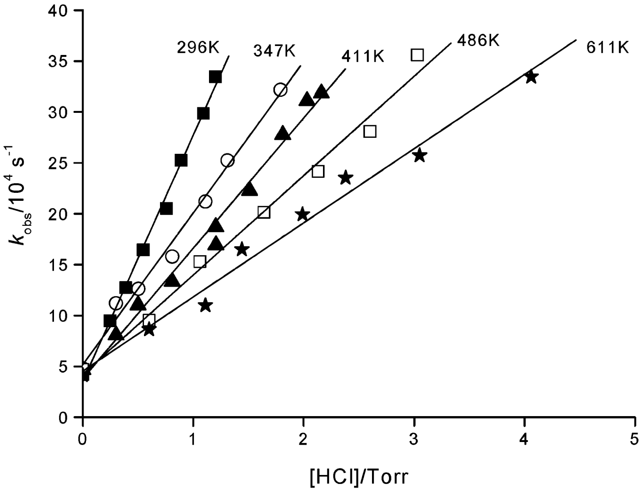

Figure 1. Second-order plots for the reaction of SiH_2 + HCl: (■) 296 K, (○) 347 K, (▲) 411 K, (□) 486 K, (★) 611 K.

TABLE 1: Experimental Second-Order Rate Constants for SiH_2 + HCl at Several Temperatures ($[SF_6]$ = 10 Torr)

T /K	k /10^{-12} cm^3 $molecule^{-1}$ s^{-1}
296	7.23 ± 0.15
347	5.39 ± 0.20
411	5.34 ± 0.18
486	4.88 ± 0.18
611	4.66 ± 0.16

TABLE 2: Pressure Dependence of Second-Order Rate Constants for SiH_2 + HCl at 296 and 611 K

P/Torr	k /10^{-12} cm^3 $molecule^{-1}$ s^{-1}
	T = 296 K
63	6.95 ± 0.70
32	6.75 ± 0.67
10	7.23 ± 0.15
3.2	6.34 ± 0.63
1.0	5.82 ± 0.58
	T = 611 K
56	5.13 ± 0.51
34	4.65 ± 0.47
10	4.66 ± 0.16
3.2	3.95 ± 0.40
1.6	4.17 ± 0.42

In addition to these experiments, some runs were carried with the total pressure (mainly SF_6) varied in the range of 1−100 Torr at the lowest and highest temperatures (296 and 611 K, respectively). The results of these runs are shown in Table 2. Error limits are higher at pressures other than 10 Torr because less experimental points were involved in obtaining these fits. The results show little variation of the rate constant values beyond reasonable experimental scatter (±10%). At both

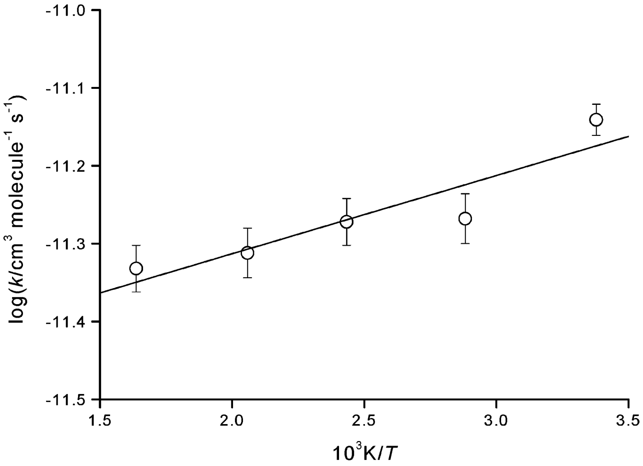

Figure 2. Arrhenius plot of the second-order rate constants for SiH_2 + HCl.

temperatures the rate constant values for pressures at and above 10 Torr are within the experimental scatter, while those below 10 Torr are slightly lower. Since the two extreme temperatures show such little effect, pressure dependence studies were not pursued at the other temperatures. Thus, the rate constants measured at 10 Torr should represent the values for the true bimolecular process. These values have been fitted to the Arrhenius equation, a plot of which is shown in Figure 2. The fit is reasonably good and the resulting equation is

$$\log(k/\mathrm{cm}^3\ \mathrm{molecule}^{-1}\ \mathrm{s}^{-1}) = (-11.51 \pm 0.06) + (1.92 \pm 0.47\ \mathrm{kJ\ mol}^{-1})/RT\ln 10$$

The slight pressure dependence observed for this reaction hints at the possibility of a third-body assisted association process. However, its small magnitude suggests that other processes may also be occurring. An explanation for this and the full mechanism lies in the underlying potential energy surface, calculations of which are described in the next section.

Ab Initio Calculations. Possible species on the SiH_3Cl potential energy surface (PES) were explored in some detail at the G3 level of theory. A fairly straightforward surface and set of species has been found. This comprises three local minima (i.e., stable intermediates or products), apart from the reactants, SiH_2 + HCl, and three transition states. The reaction pathway may be described as follows. The initial step forms the donor−acceptor complex (ylid), $H_2Si\cdots ClH$ (in syn and anti configurations), which can then either undergo a chlorine-to-silicon H-shift to form chlorosilane, SiH_3Cl^* (vibrationally excited) or decompose to give chlorosilylene by H_2 elimination (a 4-center process). The SiH_3Cl^* can then be stabilized by collisions or alternatively decompose to give HSiCl by H_2 elimination from silicon (a 3-center process). This may be summarized in the following mechanistic scheme:

$$SiH_2 + HCl \xrightarrow{1} H_2Si\cdots ClH$$

$$H_2Si\cdots ClH \xrightarrow{2} SiH_3Cl^*$$

$$H_2Si\cdots ClH \xrightarrow{3} HSiCl + H_2$$

$$SiH_3Cl^* \xrightarrow{4} HSiCl + H_2$$

$$SiH_3Cl^* + M \xrightarrow{5} SiH_3Cl$$

TABLE 3: Ab Initio (G3) Enthalpies for SiH_3Cl Species of Interest in the Reaction of SiH_2 with HCl

molecular species	energy /hartree	relative energy /kJ mol^{-1}
SiH_2 + HCl	−751.105067	0
$H_2Si\cdots ClH$ ylid-anti	−751.113650	−22.5
$H_2Si\cdots ClH$ ylid-syn	−751.113666	−22.6
TS1	−751.106188	−2.9
TS2	−751.105838	−2.0
H_3SiCl	−751.222552	−308.5
TS3	−751.116999	−31.3
H_2 + HSiCl	−751.150589	−119.5
$SiH_2Cl^\bullet + H^\bullet$	−751.076150	+75.7

TABLE 4: Molecular and Transition State Parameters for RRKM Calculations for the Decomposition of SiH_3Cl[a]

		TS complex	
parameter	molecule	TS1	TS3
wavenumber	2172 (2)	2115	2170
	2168	2105	2050
	937	1354	1530
	931(2)	986	1001
	642(2)	684	726
	510	643	691
		434	524
		186	498
A /s^{-1}		1.50×10^{14}	5.55×10^{13}
E_o /kJ mol^{-1}		306	277
Z /10^{-10} cm^3 molecule^{-1} s^{-1}		4.22	4.22

[a] Calculated at 296 K.

In this mechanism no distinction is made between the syn and anti forms of $H_2Si\cdots ClH$. Investigation of the surface between these forms showed a low maximum (TS) of 0.8 kJ mol^{-1} which means almost free rotation around the Si⋯Cl bond which connects the two forms. This also means that the IRC calculations which connect the complex to TS1 and TS2 cannot distinguish which form (conformer) links to which transition state. The structures of the intermediate species, products, and reaction transition states are shown in Figure 3 and the enthalpy values are listed in Table 3 as well as being represented on the PES in Figure 4. In addition we have also calculated the energy of the potential Cl-abstraction reaction to give chlorosilyl radical and a hydrogen atom ($^\bullet SiH_2Cl + H^\bullet$). This is included in the data in Table 3 but not shown in Figure 4 since it not competitive with the other processes identified here.

In order to throw more light on the mechanism and the issue of a third-body assisted association (i.e., the fate of SiH_3Cl^*), we have carried out RRKM calculations[31] described in the next section.

RRKM Calculations. The pressure dependence of an association reaction corresponds exactly to that of the reverse unimolecular dissociation process provided there are no other perturbing reaction channels. Although the ab initio calculations strongly suggest that there are such channels, we have carried out a calculation on the unimolecular dissociation of SiH_3Cl as a point of reference. Despite the existence of some data on the thermal decomposition of SiH_3Cl,[32] the complexity of the experimental system led us to base our calculations on parameters obtained from the ab initio calculations. Table 4 shows the vibrational wavenumbers for the molecule and the transition state TS1, for its dissociation to SiH_2 + HCl. Also listed are parameters for transition state TS3, to be discussed later. For each transition state the corresponding Arrhenius A factor and critical energy E_o are given. Although there may be uncertainties associated with these assignments, provided the A factors are reasonable and the E_o values thought to be correct, the RRKM

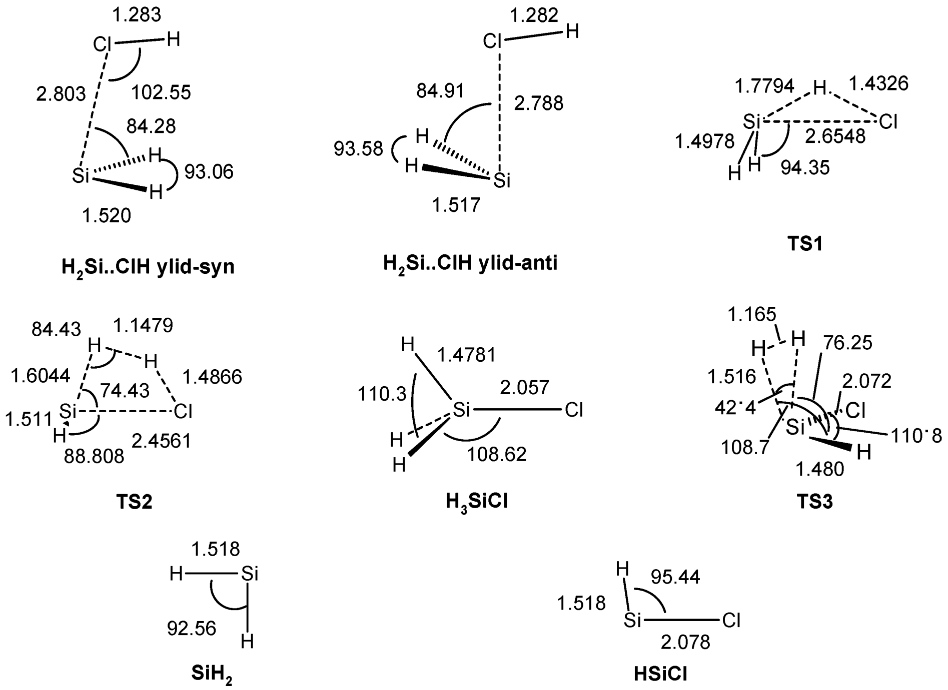

Figure 3. Ab initio MP2 = full/6-31G(d) calculated geometries of local minimum structures and transition states on the SiH_2 + HCl energy surface. Selected distances are given in Å and angles in degrees.

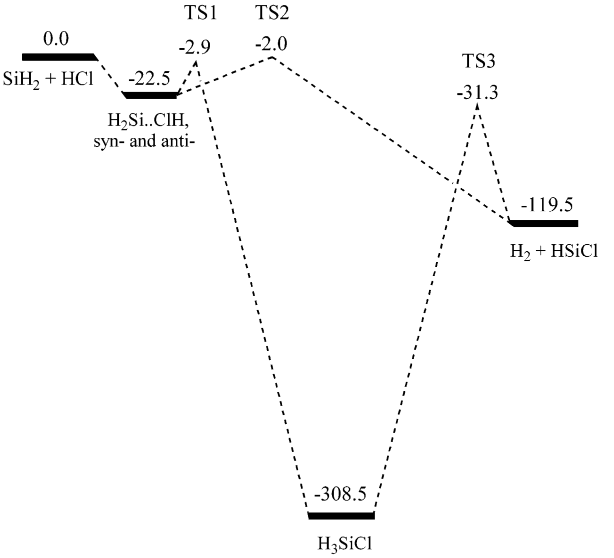

Figure 4. Potential energy (enthalpy) surface for the reaction of SiH_2 + HCl. All enthalpies (kJ mol^{-1}) are calculated at the G3 level.

TABLE 5: Predicted Pressure Dependences for the Third-Body Assisted Association Reaction SiH_2 + HCl → SiH_3Cl (in SF_6)

P/Torr	k_1/k_1^{∞} [a]
T = 296 K	
100	0.964
30	0.902
10	0.787
3	0.590
1	0.378
T = 611 K	
100	0.599
30	0.409
10	0.254
3	0.130
1	0.060

[a] Falloff relative to the high-pressure limit.

calculations are known to be reliable.[31] The calculations were carried out in conjunction with a collisional deactivation process employing a weak collisional (stepladder) model,[31] because there is considerable evidence against the strong collision assumption.[33] The average energy removal parameter, $\langle \Delta E \rangle_{down}$, which determines the collisional efficiency was taken as 12.0 kJ mol^{-1} (1000 cm^{-1}), similar to that used in previous systems with SF_6 bath gas.[6,9,11,13] The calculations were fairly insensitive to this value, since in the operational temperature range this corresponded to close to strong collisions. The results of these calculations are shown in Table 5 in terms of the so-called degree of fall-off, viz, the value of k_1/k_1^{∞} where k_1^{∞} is the true bimolecular rate constant for SiH_2 + HCl. Thus, the predictions here indicate that, at 296 K and 10 Torr pressure, the rate constant should be at 79% of its high-pressure limit falling to 38% at 1 Torr. At 611 K, the predicted fall-off is significantly greater, the rate constants being 25% at 10 Torr and 6% at 1 Torr (of the high-pressure limit). These calculations thus predict far greater pressure dependence than is observed.

This result is not surprising since it is clear from the ab initio calculations that SiH_3Cl^* can also decompose via TS3 (step 4 of the mechanism). Therefore we have also investigated the more complex system:

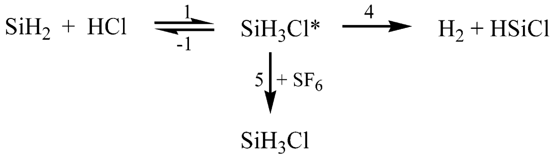

In this scheme the RRKM calculations have been employed to find the average rate constants for k_{-1} and k_4 ($\langle k_{-1} \rangle$ and $\langle k_4 \rangle$, respectively) under experimental conditions.[34] For k_4 this required the assignment shown in Table 4 for TS3. In these calculations the strong collision assumption was used. The rate constants obtained are shown in Table 6 at each of the two temperatures. It can be clearly seen that at both 296 and 611 K,

TABLE 6: RRKM Calculated Values for the Average Rate Constants for the Decomposition of SiH_3Cl^* under Experimental Conditions

P/Torr	$\langle k_{-1} \rangle$ /s^{-1} [a]	$\langle k_4 \rangle$ /s^{-1} [a]	ω /s^{-1} [b]
	$T = 296$ K		
10	4.14×10^7	1.00×10^9	1.38×10^8
3	4.14×10^7	1.00×10^9	4.14×10^7
1	4.14×10^7	1.00×10^9	1.38×10^7
	$T = 611$ K		
10	5.74×10^8	3.03×10^9	7.48×10^7
3	5.74×10^8	3.03×10^9	2.24×10^7
1	5.74×10^8	3.03×10^9	7.48×10^6

[a] Average values over the molecular energy distribution. [b] Collision frequency ($= Zp$).

TABLE 7: Comparison of Arrhenius Parameters for Selected SiH_2 Reactions[a]

reaction	log(A/cm^3 molecule^{-1} s^{-1})	E_a /kJ mol^{-1}	ref
$SiH_2 + SiH_4$	-9.91 ± 0.04	-2.1 ± 0.2	18
$SiH_2 + GeH_4$	-9.88 ± 0.02	-3.3 ± 0.3	28
$SiH_2 + C_2H_4$	-9.97 ± 0.03	-2.9 ± 0.2	25
$SiH_2 + C_2H_2$	-9.99 ± 0.03	-3.3 ± 0.2	24
$SiH_2 + Me_2CO$	-10.17 ± 0.04	-4.5 ± 0.3	9
$SiH_2 + N_2O$	-12.09 ± 0.04	-2.0 ± 0.3	12
$SiH_2 + CO_2$	-11.89 ± 0.13	16.4 ± 1.2	14
$SiH_2 + HCl$	-11.51 ± 0.06	-1.9 ± 0.5	this work

[a] High-pressure limiting values (for pressure dependent reactions).

$\langle k_4 \rangle$ is significantly larger than $\langle k_{-1} \rangle$, thus indicating that redissociation of SiH_3Cl^*, which is the cause of pressure dependence in this system is, at best, a minor process at both temperatures. The calculations suggest a 3−4% pressure dependence (viz reduction from k_1^{∞}) at 296 K and a 15−16% pressure dependence at 611 K. If a full weak collision mechanism were invoked these effects would be slightly less.[31] These effects are relatively small but comparable with those observed. It should be noted that this model does not include the direct process of H_2 elimination from the association complex (step 3 of the mechanism).

Discussion

General Comments and Rate Constant Comparisons. The main experimental purpose of the present work was to study the temperature and pressure dependence of the rate constants for the reaction of SiH_2 with HCl. This has been accomplished, and the reaction found to have a moderately high A factor and small negative activation energy. This is discussed in more detail below. Comparison with the previous study of CBEJ[16] shows that our value of the room temperature rate constant in 10 Torr SF_6, shown in Table 1, agrees well with theirs ($(7.5 \pm 1.0) \times 10^{-12}$ cm^3 molecule^{-1} s^{-1} in 9.5 Torr He). CBEJ[16] also obtained a value of $(4.3 \pm 0.6) \times 10^{-12}$ cm^3 molecule^{-1} s^{-1} in 1.0 Torr He. This suggests a rather greater pressure dependence (in He) than obtained by us (in SF_6). This is plausible since He is a weaker collision partner than SF_6. However, the effects of pressure are still small. The possible mechanistic implications are discussed later.

To try to put this study into the perspective of the range of kinetic behavior exhibited by SiH_2, a comparison of Arrhenius parameters of a variety of its reactions is shown in Table 7. The clear distinction can be drawn between the high A factor processes (log(A/cm^3 molecule^{-1} s^{-1}) in the range of −9.8 to −10.2) of SiH_4, GeH_4, C_2H_4, C_2H_2, and Me_2CO and the low A factor processes (log(A/cm^3 molecule^{-1} s^{-1}) in the range of −11.5 to −12.1) of N_2O, CO_2, and HCl. Another comparison can be made in terms of collision efficiency. We have calculated the Leonard-Jones collision numbers, Z_{LJ}, of SiH_2 with the molecules of all these reactions at 298 K and used them to work out collision efficiencies. The results, shown in Table 8, indicate the same two groupings of reactant molecules as in Table 7, with the high A factor group having collision efficiencies close to 100% whereas the low A factor group have much lower efficiencies. CO_2 is exceptionally low because it also has (unusually for SiH_2 reactions) a positive activation energy. These divisions do not per se depend on the reaction type. The efficient group includes bond insertion processes (SiH_4, GeH_4), π-type additions (C_2H_4, C_2H_2), and reactions with lone pair donors (Me_2CO). The less efficient group involves (at the moment) only reactions with lone pairs (N_2O, CO_2, and HCl). The underlying feature which distinguishes between these two groups is the secondary barrier to reaction. In $SiH_2 + CO_2$ (and now $SiH_2 + HCl$) the barrier to rearrangement of the initial complex is high enough to make the second step rate determining. (For $SiH_2 + N_2O$ the energy surface is unknown.) The secondary barrier does not have to be positive to do this (although it is for CO_2) since the secondary processes involve tight transition states which therefore cause bottlenecks (sometimes called entropy bottlenecks). To verify this for the present case, we have used the ab initio calculations to estimate the entropies of TS1 (270 J K^{-1} mol^{-1}) and TS2 (264 J K^{-1} mol^{-1}) from their calculated structures and vibrational wavenumbers. We have then used the transition state theory expression ($A = e^2(kT/h) \exp(\Delta S^{\ddagger}/R)$)[35] to calculate log($A$/$cm^3$ molecule$-^1$ s^{-1}) values of −11.82 and −12.13 for reaction via TS1 and TS2, respectively (using also calculated entropies for SiH_2 and HCl). Although these values do not quite match the experimental one (−11.51) they are sufficiently close (a factor of 2 for TS1) to support the idea that passage through one or the other (or both) of TS1 and TS2 are rate controlling. The measured negative activation energy is also close to the calculated values for these transition states. Thus it appears to us that the donor−acceptor complex (in either syn or anti form) does not affect the kinetics of this reaction, except as a stepping stone to the transition states. This is partly a consequence of its weak binding energy and stands in complete contrast to the SiH_2 and H_2O reaction where the complex is the final product.[5,6]

TABLE 8: Lennard-Jones Collision Efficiencies at 298 K for Selected Reactions of SiH_2

reaction partner	k[a]	Z_{LJ}[a,b]	efficiency(%)
SiH_4	4.60[c]	4.60	100
GeH_4	3.06[d]	4.14	74
C_2H_4	3.5[e]	4.92	71
C_2H_2	4.0[f]	4.90	82
Me_2CO	4.2[g]	5.54	76
N_2O	0.019[h]	4.12	0.46
CO_2	$<4.2 \times 10^{-5}$[i]	4.10	$<1.02 \times 10^{-3}$
HCl	0.0723[j]	4.04	1.79

[a] High-pressure limiting values, units: 10^{-10} cm^3 molecule^{-1} s^{-1}. [b] The procedure for calculating Z_{LJ} is described in ref 29. Parameters were taken from refs 29, 38, and 39. [c] Reference 18. [d] Reference 29. [e] Reference 26. [f] Reference 25. [g] Reference 9. [h] Reference 12. [i] Reference 14. [j] This work.

Ab Initio Calculations, RRKM Calculations, and the Mechanism. The early theoretical calculations of RCGD[4] revealed the donor−acceptor complex at −8 kJ mol^{-1} and TS1 at +25 kJ mol^{-1} relative to SiH_2 and HCl. Su and Schlegel[17] obtained well depths of between 6.3 and 19.7 kJ mol^{-1} (including ΔZPE) and barriers (TS1) in the range of −4.6 to +28.9 kJ mol^{-1}, depending on the level of calculation and basis set used. Our calculations are in quite close agreement with

TABLE 9: Quantum Chemical Calculated Energy Barriers (in kJ mol^{-1}) for Chlorosilane Decomposition Pathways

decomposition pathway	this work	Raghavachari et al.[a]	Su and Schlegel[b]	Walch and Dateo[c]
$SiH_3Cl \rightarrow SiHCl + H_2$	277		280	279
$SiH_3Cl \rightarrow SiH_2 + HCl$	305	314	318	322

[a] Reference 4. [b] Reference 17. [c] Reference 36.

those of Su and Schlegel[17] at the MP2/6-311++G(3df,3pd) level, with a relatively deep well and a small negative barrier. The crucial point is that TS1 lies 3 kJ mol^{-1} below the reactants. A positive energy for TS1 would not be consistent with the observed reaction kinetics. A new feature of this PES is the direct route (step 3) from complex $H_2Si\cdots ClH$) to products ($HSiCl + H_2$) via TS2, a pathway not previously identified (either theoretically or experimentally) in this system. The analogue of this pathway, however, has been shown to exist in the SiH_2 and H_2O reaction leading from $H_2Si\cdots OH_2$ to HSiOH $+ H_2$.[5,6] It is not possible to say from the results of the present study whether TS1 or TS2 is the dominant rate determining step, as they are extremely close in energy. TS2 has the tighter structure (lower entropy) which suggests that step 2 of the reaction scheme (via TS1) may be the more important pathway. For product determination it hardly matters since step 2 (via TS1) leads to chemically activated SiH_3Cl at circa 28 kJ mol^{-1} above the threshold barrier (TS3) for formation of HSiCl and H_2. The RRKM calculations indicate that the slight pressure dependence found in our experiments is not consistent with that of a third-body assisted association since the calculated extents of fall-off (at both 296 and 611 K) were much greater than those found. When the RRKM calculations were extended to include decomposition of SiH_3Cl^* via TS3, a much diminished pressure dependence was found more in keeping with the experimental findings and also those of CBEJ.[16] This arises because the large bulk of SiH_3Cl^* decomposes via TS3 (step 4) and very little redissociates to reactants via TS1. The calculated trend is still, however, to show increased pressure dependence with increasing temperature. The measured effects do not support this, although the scatter in the data could mask it. These calculations still leave open to some extent the question of the contribution of step 3. Although the direct process of H_2 formation by this pathway is pressure independent, the ab initio calculations show that it could compete. The difficulty of the results is that if this pathway was dominant there would be no pressure dependence, whereas for it to provide a best fit would require the importance of step 3 to increase with temperature in order to offset the increased pressure dependence predicted (from steps 1, −1, 4 and 5) at higher temperature. The energy surface and the *A* factor calculations do not support this. Thus, we are uncertain of the relative importance of the two routes leading to final products.

Our calculations may also be compared with those of other studies [4,17,36] concerned with the thermal decomposition of SiH_3Cl. Table 9 shows this comparison of the barriers to decomposition of SiH_3Cl via the two possible silylene formation pathways. For both available channels the values for the decomposition barriers are in good agreement despite the differences in calculation levels. This lends confidence to these results. The most recent experimental value for the decomposition barrier of SiH_3Cl (to $HSiCl + H_2$) is 254 ± 8 kJ mol^{-1}. This comes from a study of the thermal decomposition of SiH_3Cl by Ring, O'Neal, and co-workers.[32] It should be added that the complexity of the overall mechanism of SiH_3Cl decomposition must add a further element of uncertainty to this value.

There seems to be strong evidence that silylenes are involved in the direct synthesis of methylchlorosilanes.[37] Although the particular silylenes implicated are $SiCl_2$ and MeSiCl, the importance of the work presented here is that it provides a framework of reference for the kinetics and mechanisms of reactions of silylene with chlorinated species.

Acknowledgment. R.B. and R.W. thank Dow-Corning for a Grant in support of the experimental work. R.B. also thanks the Spanish DGI for support under project BQU2002-03381.

References and Notes

(1) Jasinski, J. M.; Becerra, R.; Walsh, R. *Chem. Rev.* **1995**, *95*, 1203.
(2) Becerra, R.; Walsh, R. Kinetics & Mechanisms of Silylene Reactions: A Prototype for Gas-Phase Acid/Base Chemistry. In *Research in Chemical Kinetics*; Compton, R. G., Hancock, G., Eds.; Elsevier: Amsterdam, 1995; Vol. 3, p 263.
(3) Gaspar, P. P.; West, R. Silylenes. In *The Chemistry of Organic Silicon Compounds*; Rappoport, Z., Apeloig, Y., Eds.; Wiley: Chichester, U.K., 1998; Vol. 2, Chapter 43, p 2463.
(4) Raghavachari, K.; Chandrasekhar, J.; Gordon, M. S.; Dykema, K. J. *J. Am. Chem. Soc.* **1984**, *106*, 5853.
(5) Alexander, U. N.; King, K. D.; Lawrance, W. D. *J. Phys. Chem. A* **2002**, *106*, 973.
(6) Becerra, R.; Cannady, J. P.; Walsh, R. *J. Phys. Chem. A* **2003**, *107*, 11049.
(7) Becerra, R.; Carpenter, I. W.; Gutsche, G. J.; King, K. D.; Lawrance, W. D.; Staker, W. S.; Walsh, R. *Chem. Phys. Lett.* **2001**, *333*, 83.
(8) Alexander, U. N.; King, K. D.; Lawrance, W. D. *Phys. Chem. Chem. Phys.* **2001**, *3*, 3085.
(9) Becerra, R.; Cannady, J. P.; Walsh, R. *J. Phys. Chem. A* **1999**, *103*, 4457.
(10) Becerra, R.; Cannady, J. P.; Walsh, R. *Phys. Chem. Chem. Phys.* **2001**, *3*, 2343.
(11) Becerra, R.; Cannady, J. P.; Walsh, R. *J. Phys. Chem. A* **2002**, *106*, 11558.
(12) Becerra, R.; Frey, H. M.; Mason, B. P.; Walsh, R. *Chem. Phys. Lett.* **1991**, *185*, 415.
(13) Becerra, R.; Cannady, J. P.; Walsh, R. *J. Phys. Chem. A* **2001**, *105*, 1897.
(14) Becerra, R.; Cannady, J. P.; Walsh, R. *J. Phys. Chem. A* **2002**, *106*, 4922.
(15) Rochow, E. G. *Silicon and Silicones*; Springer-Verlag: Berlin, 1987.
(16) Chu, J. O.; Beach, D. B.; Estes, R. D.; Jasinski, J. M. *Chem. Phys. Lett.* **1988**, *143*, 135.
(17) Su, M.-D.; Schlegel, H. B. *J. Phys. Chem. A* **1993**, *97*, 9981.
(18) Becerra, R.; Frey, H. M.; Mason, B. P.; Walsh, R.; Gordon, M. S. *J. Chem. Soc., Faraday Trans.* **1995**, *91*, 2723.
(19) Baggott, J. E.; Frey, H. M.; King, K. D.; Lightfoot, P. D.; Walsh, R.; Watts, I. M. *J. Phys. Chem.* **1988**, *92*, 4025.
(20) Jasinski, J. M.; Chu, J. O. *J. Chem. Phys.* **1988**, *88*, 1678.
(21) Frisch, M. J.; Trucks, G. W.; Schlegel, H. B.; Scuseria, G. E.; Robb, M. A.; Cheeseman, J. R.; Zakrzewski, V. G.; Montgomery, J. A., Jr.; Stratmann, R. E.; Burant, J. C.; Dapprich, S.; Millam, J. M.; Daniels, A. D.; Kudin, K. N.; Strain, M. C.; Farkas, O.; Tomasi, J.; Barone, V.; Cossi, M.; Cammi, R.; Mennucci, B.; Pomelli, C.; Adamo, C.; Clifford, S.; Ochterski, J.; Petersson, G. A.; Ayala, P. Y.; Cui, Q.; Morokuma, K.; Malick, D. K.; Rabuck, A. D.; Raghavachari, K.; Foresman, J. B.; Cioslowski, J.; Ortiz, J. V.; Baboul, A. G.; Stefanov, B. B.; Liu, G.; Liashenko, A.; Piskorz, P.; Komaromi, I.; Gomperts, R.; Martin, R. L.; Fox, D. J.; Keith, T.; Al-Laham, M. A.; Peng, C. Y.; Nanayakkara, A.; Gonzalez, C.; Challacombe, M.; Gill, P. M. W.; Johnson, B. G.; Chen, W.; Wong, M. W.; Andres, J. L.; Head-Gordon, M.; Replogle, E. S.; Pople, J. A. *Gaussian 98*, revision A.9; Gaussian, Inc.: Pittsburgh, PA, 1998.
(22) Curtiss, L. A.; Raghavachari, K.; Redfern, P. C.; Rassolov, V.; Pople, J. A. *J. Chem. Phys.* **1998**, *109*, 7764.
(23) Gonzales, C.; Schlegel, H. B. *J. Chem. Phys.* **1989**, *90*, 2154.
(24) Pople, J. A.; Scott, A. P.; Wong, M. W.; Radom, L. *Isr. J. Chem.* **1993**, *33*, 345.
(25) Becerra, R.; Walsh, R. *Int. J. Chem. Kinet.* **1994**, *26*, 45.
(26) Al-Rubaiey, N.; Walsh, R. *J. Phys. Chem.* **1994**, *98*, 5303.
(27) Becerra, R.; Frey, H. M.; Mason, B. P.; Walsh, R. *J. Organomet. Chem.* **1996**, *521*, 343.
(28) Al-Rubaiey, N.; Carpenter, I. W.; Walsh, R.; Becerra, R.; Gordon, M. S. *J. Phys. Chem. A* **1998**, *102*, 8564.
(29) Becerra, R.; Boganov, S.; Walsh, R. *J. Chem. Soc., Faraday Trans.* **1998**, *94*, 3569.
(30) Al-Rubaiey, N.; Becerra, R.; Walsh, R. *Phys. Chem. Chem. Phys.* **2002**, *4*, 5072.
(31) Holbrook, K. A.; Pilling, M. J.; Robertson, S. H. *Unimolecular Reactions*, 2nd ed.; Wiley: Chichester, U.K., 1996.

(32) Walker, K. L.; Jardine, R. E.; Ring, M. A.; O'Neal, H. E. *Int. J. Chem. Kinet.* **1998**, *30*, 69.

(33) Hippler, H.; Troe, J. In *Advances in Gas-Phase Photochemistry and Kinetics*; Ashfold, M. N. R., Baggott, J. E., Eds.; Royal Society of Chemistry: London, 1989; Vol. 2, Chapter 5, p 209.

(34) The average rate constants for each pathway i, $\langle k_i \rangle$ were computed via $\langle k_i \rangle = \sum_j n_j k_{ij}(E)$ where n_j is the fractional population and $k_{ij}(E)$ is the microcanonical rate constant of the jth level of pathway i.[31]

(35) Benson, S. W. *Thermochemical Kinetics*, 2nd ed.; Wiley: New York, 1976.

(36) Walch, S. P.; Dateo, C. E. *J. Phys. Chem. A* **2001**, *105*, 2015.

(37) Clarke, M. P.; Davidson, I. M. T. *J. Organomet. Chem.* **1991**, *408*, 149.

(38) Becerra, R.; Walsh, R. *J. Organomet. Chem.* **2001**, *636*, 49.

(39) Reid, R. C.; Prausnitz, J. M.; Poling, B. E. *The Properties of Gases and Liquids*, 4th ed.; McGraw-Hill: New York, 1988.